Voltage Sensing by Fluorescence Resonance Energy Transfer in Single Cells

Jesús E. González and Roger Y. Tsien
Howard Hughes Medical Institute, University of California, San Diego, La Jolla, California 92093-0647 USA

ABSTRACT A new mechanism has been developed for achieving fast ratiometric voltage-sensitive fluorescence changes in single cells using fluorescence resonance energy transfer. The mechanism is based on hydrophobic fluorescent anions that rapidly redistribute from one face of the plasma membrane to the other according to the Nernst equation. A voltage-sensitive fluorescent readout is created by labeling the extracellular surface of the cell with a second fluorophore, here a fluorescently labeled lectin, that can undergo energy transfer with the membrane-bound sensor. Fluorescence resonance energy transfer between the two fluorophores is disrupted when the membrane potential is depolarized, because the anion is pulled to the intracellular surface of the plasma membrane far from the lectin. Bis-(1,3-dialkyl-2-thiobarbiturate)-trimethineoxonols, where alkyl is *n*-hexyl and *n*-decyl (DiSBA-C_6-(3) and DiSBA-C_{10}-(3), respectively) can function as donors to Texas Red labeled wheat germ agglutinin (TR-WGA) and acceptors from fluorescein-labeled lectin (Fl-WGA). In voltage-clamped fibroblasts, the translocation of these oxonols is measured as a displacement current with a time constant of ~2 ms for 100 mV depolarization at 20°C, which equals the speed of the fluorescence changes. Fluorescence ratio changes of between 4% and 34% were observed for a 100-mV depolarization in fibroblasts, astrocytoma cells, beating cardiac myocytes, and B104 neuroblastoma cells. The large fluorescence changes allow high-speed confocal imaging.

INTRODUCTION

Fluorescence detection and imaging of cellular electrical activity is a technique of great importance and potential (for recent reviews see Grinvald et al., 1988; Salzberg, 1983; Cohen and Lesher, 1985). Mechanisms for optical sensing of membrane potential have traditionally been divided into two classes: sensitive but slow redistribution of permeant ions from extracellular medium into the cell, and fast but small perturbations of relatively impermeable dyes attached to one face of the plasma membrane (Loew, 1988, 1993; Waggoner and Grinvald, 1977). The permeant ions are sensitive because the ratio of their concentrations between the inside and outside of the cell can change by up to the Nernstian limit of 10-fold for 60 mV change in transmembrane potential. Their responses are slow because to establish new equilibria, ions must diffuse through unstirred layers in each aqueous phase and the low-dielectric-constant interior of the plasma membrane. By contrast, the impermeable dyes can respond very quickly because they need little or no translocation, but they are insensitive because they sense the electric field with only a part of a unit charge moving less than the length of the molecule, which in turn is only a small fraction of the distance across the membrane. Furthermore, a significant fraction of the total dye signal comes from molecules that sit on irrelevant membranes or cells and that dilute the signal from the few correctly placed molecules.

Received for publication 7 April 1995 and in final form 11 July 1995.

Address reprint requests to Dr. Roger Y. Tsien, Howard Hughes Medical Institute, University of California, San Diego, 310 Cellular & Molecular Medicine West, 9500 Gilman Drive, La Jolla, CA 92093-0647. Tel.: 619-534-4891; Fax: 619-534-5270; E-mail: rtsien@ucsd.edu.

0006-3495/95/10/1272/09 $2.00

In this work, we have attempted to combine the best features of the above two types of mechanisms. To achieve high sensitivity, the voltage sensor should translocate at least a full unit charge nearly all the way through the membrane. Even without specific ion channels or transporters, such translocation can be quite rapid if the ion is negatively charged, delocalized, and hydrophobic. For example, the lipid-soluble anion of dipicrylamine (2,2′,4,4′,6,6′-hexanitrodiphenylamine) produces displacement currents in excitable tissue with submillisecond kinetics, comparable in speed to sodium channel gating currents (Benz and Conti, 1981; Benz and Nonner, 1981; Fernández et al. 1983). However, voltage sensing should not require further diffusion of the ion through the unstirred aqueous layers, because that slows the response tremendously and generates a sustained leakage current. But how can one create an optical readout from the translocation of a membrane-bound ion merely from one side of the plasma membrane to the other side? We choose to use fluorescence resonance energy transfer (FRET) between the translocating ions and fluorophores fixed to just one face of the plasma membrane, most conveniently the extracellular face. For example, suppose the translocating ions are anionic fluorescent acceptors that absorb at wavelengths that overlap with the emission spectrum of the extracellularly fixed donor fluorophores, as schematically shown in Fig. 1. At normal negative membrane potentials, most of the permeant anions will be on the extracellular face of the plasma membrane, where they can get close enough to the donors so that excited state energy can be transferred to the membrane-bound acceptors. Upon depolarization, the acceptor anions will translocate to the intracellular face of the membrane, greatly increasing their mean distance from the donors, reducing the probability of energy transfer and generating a

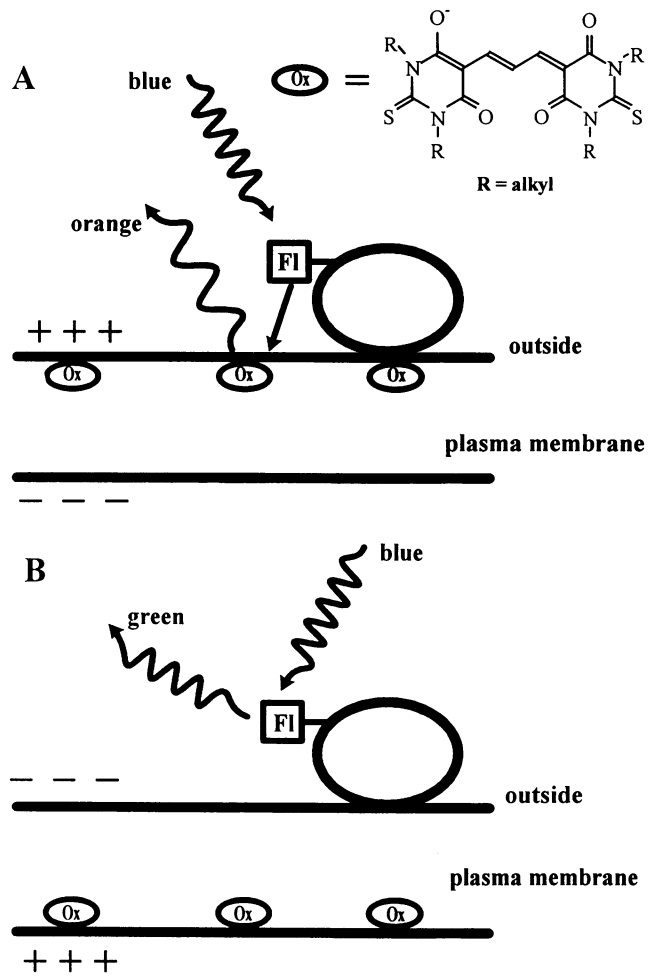

FIGURE 1 A scheme of the voltage-sensitive FRET mechanism. At a resting negative membrane potential (*A*) the permeable oxonols have a high concentration at the extracellular surface of the plasma membrane and energy transfer from the extracellularly bound FL-WGA is favored. FRET is symbolized as the straight arrow from lectin to oxonol. At a positive membrane potential (*B*) the anions are located primarily on the intracellular surface of the membrane and energy transfer is greatly reduced because of the increased mean distance from the donors on the extracellular surface. The generic structure of the oxonols is shown in the top right corner.

shift in intensity from acceptor to donor wavelengths. The speed of the voltage response depends on the translocation rate of the fluorophore from one site to the other. In principle, the permeant ions could be the donors rather than the acceptors; each of the alternatives has its own advantages.

The permeant ions have to satisfy numerous molecular requirements. They must be highly hydrophobic with a single delocalized charge to bind strongly to the plasma membrane and translocate rapidly across it in response to membrane potential. Delocalization of the charge reduces the Born charging energy (inversely proportional to radius) for moving a charged molecule from a hydrophilic to a hydrophobic environment and is essential for rapid translocation of ions (Benz, 1988). Increasing hydrophobicity minimizes release of the bound dye from the plasma membrane and buries the ion deeper in the membrane, which decreases the electrostatic activation energy for translocation. Polar groups on the ion should be kept to a minimum and shielded as much as possible to disfavor solvation in the headgroup region of the bilayer. However, hydrophobicity cannot be increased without limit, because some aqueous solubility is required to permit cellular loading. Anions have a tremendous inherent speed advantage over cations, because the ester groups of biological membranes generate a sizable dipole potential within the hydrocarbon core of the membrane. This potential aids anion translocation through the hydrophobic layer but hinders cations. It is known that for the isostructural ions tetraphenyl phosphonium cation and tetraphenylborate anion, the anion is much more permeable than the cation (Flewelling and Hubbell, 1986). Ideally, the time constants for translocation should be less than a millisecond to permit single action potentials to be monitored. However, somewhat slower kinetics are not completely disqualifying, because many practical optical recordings from complex neuronal systems, especially CNS preparations, do not attempt to resolve single action potentials. The anions must be strongly fluorescent when adsorbed to the membrane, whereas they should have minimal fluorescence when free in aqueous solution. They should not act as ionophores, especially protonophores, because such behavior would generate sustained leakage currents far more injurious than the unavoidable transient displacement currents. Therefore any protonation pK_a must be kept far below 7. Ultimately, red to infrared wavelengths of excitation and emission will be preferred, to avoid tissue scattering and heme absorbances. Photodynamic damage must be kept as low as possible; this is probably best done by minimizing triplet state formation and the resulting generation of singlet oxygen.

MATERIALS AND METHODS

Chemistry

All starting materials and reagents were of the highest purity available (Aldrich; Milwaukee, WI) and were used without further purification, except where noted. Solvents were HPLC grade (Fisher) and were dried over activated molecular sieves (3 Å). NMR spectra were acquired on a Varian Gemini 200 MHz spectrometer (Palo Alto, CA). The spectra were referenced relative to the residual solvent peak ($CHCl_3$, δ = 7.24 ppm). Fluorescence spectra were taken on a SPEX Fluorolog-2 (Edison, NJ) and were corrected for lamp and detector wavelength variations using the manufacturer-supplied correction files.

DiSBA-C_4-(3) was synthesized based on the procedure for the ethyl derivative (Tsien, 1976). 1,3-Di-butyl-thiobarbiturate (500 mg, 2 mmol) was dissolved in 700 μl of pyridine. To this solution, a mixture of 181 μl (1.1 mmol) of malonaldehyde bis(dimethyl acetal) and 100 μl of 1 M HCl was added. The solution immediately turned red. After 3 h, half of the reaction mixture was removed and 2 equiv. of the protected malonaldehyde was added every hour for 4 h to the remaining mixture. The reaction mixture was then filtered to collect purple/black crystals of the DiSBA-C_4-(3) pyridinium salt. After washing the crystals with water and then drying under vacuum (0.5 torr), 67.2 mg of pure product was collected. ^1H NMR ($CDCl_3$): δ 8.91 (2H, d, J = 5.1 Hz, py), 8.76 (1H, t, J = 13.7 Hz, central methine), 8.52 (1H, t, J = 8.0 Hz, py), 8.16 (2H, d, J = 13.9 Hz, methine), 8.00 (2H, dd, $J_1 \sim J_2$ = 6.9 Hz, py), 4.47 (8H, cm,

$NCH_2CH_2CH_2CH_3$), 1.69 (8H, cm, $NCH_2CH_2CH_2CH_3$), 1.39 (8H, cm, $NCH_2CH_2CH_2CH_3$), 0.95 (12H, t, J = 6.4 Hz, methyl).

1,3-Di-butyl-thiobarbiturate: 1.22 g of Na (53 mmol) was slowly dissolved in 20 ml of dry ethanol under argon. To the ethoxide solution, 8.5 g (8 ml, 53 mmol) of diethyl malonate followed by 5 g (26.5 mmol) of dibutylthiourea was added. The reaction mixture was heated and refluxed for 3 days. After cooling, the mixture was filtered. The filtrate was clarified with addition of water. Concentrated HCl was then added until the pH was 1–2. The acidic filtrate was then extracted three times with hexanes. The extract was concentrated and 5.5 g of crude product precipitated out of solution. The solid was recrystallized from methanol with the addition of a small amount of water, yielding 4.23 g of the pure barbituric acid (65%). ^{1}H NMR ($CDCl_3$): δ 4.33 (4H, cm, $NCH_2CH_2CH_2CH_3$), 3.71 (2H, s, ring CH_2), 1.63 (4H, cm, $NCH_2CH_2CH_2CH_3$), 1.35 (4H, cm, $NCH_2CH_2CH_2CH_3$), 0.94 (6H, t, J = 6.2 Hz, methyl). Other oxonols were made using the same procedure, starting with the appropriate thiourea (prepared from requisite primary amine and carbon disulfide) (Bortnick et al. 1956). All of the oxonols described have similar NMR spectra. The only differences are the integrations of the alkyl substituents and presence of different counter-ions if ion exchanged. FL-WGA was purchased from Sigma Chemical Co. (St. Louis, MO). TR-WGA was prepared from WGA and Texas Red (Molecular Probes; Eugene, OR) in a 100 mM bicine buffer at pH 8.5. A 73 μM solution of WGA was reacted with a sixfold excess of Texas Red for 1 h at room temperature. The protein conjugate was purified on a G-25 Sephadex column.

Cells and staining

All cells were grown and handled like L-M(TK$^-$) ones except where noted. L-M(TK$^-$) cells were grown in Dulbecco's modified Eagle's media (Gibco; Grand Island, NY) with 10% fetal bovine serum and 1% penicillin streptomycin (Gemini; Calabasas, CA). B104 cells were differentiated with 1 μM retinoic acid for 5 days before use. The cells were plated on glass coverslips at least 1 day before use. The adherent cells were washed and maintained in 2.5–3.0 ml of Hanks' balanced salt solution (HBSS) with 1 g/L glucose and 20 mM HEPES at pH 7.4. A freshly prepared 75 μM aqueous solution of the appropriate oxonol was made before an experiment from a DMSO stock solution. The cells were stained by mixing 100 μl of the oxonol solution with 750 μl of the bath and then adding the diluted solution to the cells. The dye was left for 30–40 min at a bath concentration of 2.3 μM. β-Cyclodextrin (1.5 mM) in the bath solution was necessary for cell loading of DiSBA-C_6-(3). The butyl and ethyl derivatives were water-soluble enough to load cells without β-cyclodextrin complexation. DiSBA-C_{10}-(3) was loaded in a pH 7.4 solution containing 290 mM sucrose and 10 mM HEPES, 364 mOsm, for 10 min at a bath concentration of 10 μM. DiSBA-C_{10}-(3) labeling was quenched by replacing the bath with HBSS solution. The cells were stained with 15 μg/ml of FL-WGA for 15 min. The B104 cells required a 125 μg/ml bath concentration to give satisfactory lectin staining. The excess dyes were removed with repeated washes with HBSS. If the excess ethyl or butyl oxonol derivatives were left in the bath, slow currents and fluorescence changes due to redistribution of the dyes into the cell were observed during depolarizations greater than 1 s. The cardiac myocytes (Henderson et al., 1989) were a gift of Professor Kenneth Chien, UCSD. The Jurkat lymphocyte suspensions were grown in RPMI media with 5% heat-inactivated fetal bovine serum and 1% of a 10,000 U/mL and 10,000 μg/mL penicillin streptomycin solution. Aliquots (15–20 ml) of the cellular suspension were washed three times before and after dye staining by centrifugation at 100 $\times$ g for 4 min followed by additions of fresh HBSS.

Optical recordings

The fluorescently labeled cells were excited with light from a 75-W xenon lamp passed through 450–490 nm excitation interference filters. The light was reflected onto the sample using a 505-nm dichroic. The emitted light was collected with a 63X Zeiss (1.25 or 1.4 numerical aperture) lens, passed through a 505-nm long-pass filter and directed to a G-1B 550-nm dichroic (Nikon; Melville, NY). The reflected light from this second dichroic was passed through a 515 DF35 bandpass filter and made up the FL-WGA signal. The transmitted light was passed through a 560 or 570 LP filter and comprised the oxonol signal. For experiments using the oxonol as a donor to TR-WGA, the 550-nm dichroic was used for excitation and a 580-nm dichroic was used to split the emission. The long-wavelength Texas Red fluorescence was passed through a 605-nm DF55 bandpass filter. Voltage-dependent fluorescence changes in single cells were measured using a Nikon microscope attached to a Photoscan II photometer equipped with two R928 PMTs for dual-emission recordings. A 7-point Savitsky-Golay smoothing routine was applied to all optical data (Savitzky and Golay, 1964), unless otherwise noted. The 1–2 KHz single wavelength data was acquired with an Axobasic program that used the TTL pulse counting routine LEVOKE. The confocal image was acquired using a home-built, high-speed confocal microscope (Tsien and Bacskai, 1994). The cell was voltage-clamped at a holding potential of -70 mV. After a 200-ms delay, the cell was given a 200-ms depolarizing square voltage pulse to 50 mV. Images were collected every 67 ms. The second and fifth images are shown in the figure and are the average of 16 responses.

Electrophysiology

Patch clamp recordings were made using an Axopatch 1-D amplifier equipped with a CV-4 headstage from Axon Instruments (Foster City, CA). The data were digitized and stored using the PCLAMP software. The pH 7.4 intracellular solution used contained 125 mM potassium gluconate, 1 mM $CaCl_2 \cdot 2H_2O$, 2 mM $MgCl_2 \cdot 6H_2O$, 11 mM EGTA, and 10 mM HEPES. For the B104 cells, 4 mM ATP and 0.5 mM GTP were added.

Calculations and equation fits

The quantum yield of DiSBA-C_6-(3) was determined relative to rhodamine B in ethanol (Φ_F = 0.97) (Weber and Teale, 1957). R_o was calculated following standard procedures (Wu and Brand, 1994). The spectra of FL-WGA in HBSS and DiSBA-C_6-(3) in octanol were used to determine the overlap integral. Values of 1.4 and 0.67 were used for the index of refraction and orientation factor, respectively.

The fits to the equations were done using the Marquardt-Levenberg least-squares algorithm within the commercial program Sigmaplot (Jandel Scientific, San Rafael, CA).

RESULTS AND DISCUSSION

Rapid translocation of a fluorescent anion

Symmetrical bis(thiobarbiturate)oxonols were chosen as likely candidates for rapidly translocating fluorescent ions based on the above design criteria. The strong absorbance maximum ($\epsilon \sim$ 200,000 M^{-1} cm^{-1}) at 540 nm and good quantum yield (0.40) in membranes makes them desirable for use as a fluorescence donors or acceptors in cells. The fluorescence excitation and emission spectra of DiSBA-C_6-(3) is shown in Fig. 2 along with those for FL-WGA and TR-WGA. Another extremely useful property of these oxonols is that their fluorescence emission maximum at 560 nm is 20 times brighter when bound to membranes than in aqueous solution (Rink et al., 1980). Furthermore, the negative charge is delocalized throughout the chromophore, with the four equivalent oxygens containing the majority of the charge. The high electron affinity of the thiobarbiturate moieties discourages protonation ($pK_a < 1$) and resists photooxidative bleaching. The four *N*-alkyl groups and the

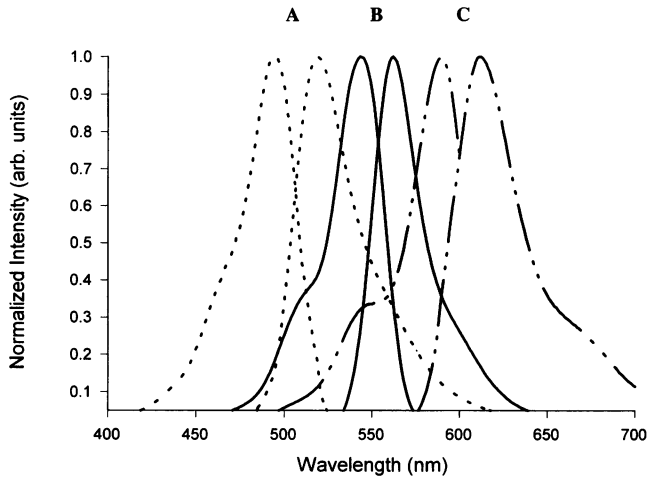

FIGURE 2 Normalized excitation and emission spectra for (*A*) FL-WGA in HBSS (- - - -), (*B*) DiSBA-C_6-(3) in octanol (—), and (*C*) TR-WGA in HBSS (- - — - - -). The excitation spectra are the shorter of each pair. Octanol was selected as the oxonol solvent in order to mimic the membrane environment.

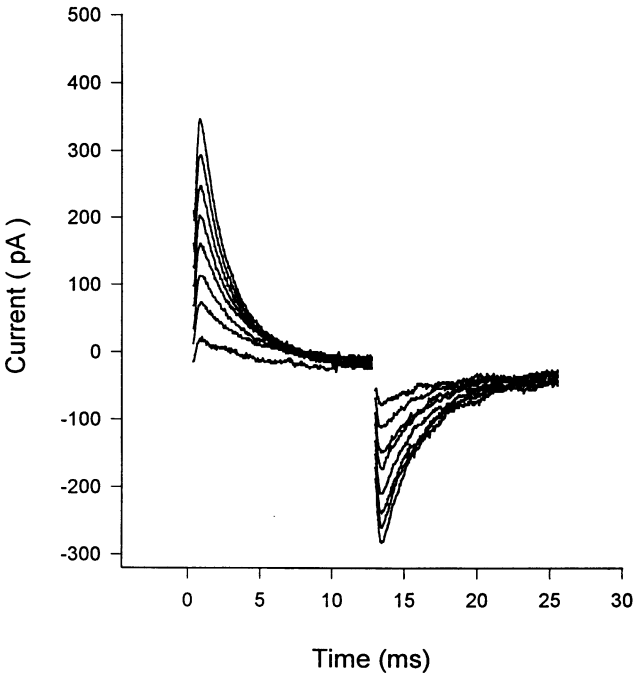

FIGURE 3 Displacement and tail currents of L-M(TK$^-$) cells stained with 2.3 μM DiSBA-C_6-(3) at 20°C. 12.5-ms long voltage steps at 15-mV increments were applied to the cell, from a holding potential of −70 mV. The larger, faster transients due to simple membrane capacitance transient could be minimized using the capacitance and series resistance compensation capabilities of the Axopatch amplifier. These control currents in cells without dye have decayed to <25 pA by 300 μs for the largest depolarization step of 120 mV and are proportionately less for smaller voltage changes.

thiocarbonyl give the molecule the necessary amount of hydrophobicity needed for tight membrane binding and rapid translocation. The translocation rates were studied in L-M(TK$^-$) cells using whole-cell voltage clamp recording. The L-M(TK$^-$) cells were chosen because they have very low background currents and are easy to patch clamp. These cells have a resting potential of −5 mV and no obvious voltage activated currents. Displacement currents from DiSBA-C_6-(3) at 20°C are displayed in Fig. 3. The currents are due to redistribution of the membrane-bound oxonol in response to 8 depolarizations. The time constant for the displacement current is 2 ms for 120 mV depolarization. Equal amounts of charge move at the onset and conclusion of the voltage step, but in opposite directions, consistent with redistribution of stored ions from one energy minimum to the other across the plasma membrane. Furthermore, the induced capacitance dq/dV from the oxonol movement is calculated to be ~5 pF for 100 mV depolarization. This value corresponds to roughly one-third the membrane capacitance without the dye. Interestingly, sodium channel gating charges are also responsible for about 33% of the total capacitance of squid axons for small depolarizations (Hodgkin, 1975). Negligible currents were observed in the absence of the oxonol. DiSBA-C_{10}-(3) gave displacement currents of approximately the same speed, whereas analogues with R = butyl and ethyl gave much slower currents. The butyl compound had a time constant of ~18 ms and the currents from the ethyl compound were very small, slow, and difficult to observe. Figs. 4 and 5 show the voltage dependence and time constants for charge translocation in a cell loaded with about 4 times as much oxonol as in the experiment of Fig. 3. The experimental data are in reasonable accord with existing models of hydrophobic ion transport between two energy minima near the aqueous interfaces of the lipid bilayer (Ketterer et al., 1971; Andersen and Fuchs, 1975; Benz et al., 1976). These models predict that the equilibrium charge displacement $\Delta q(V)$ and the translocation time constant $\tau(V)$ should depend on the externally applied membrane potential V in the following manner:

$$\Delta q(V) = \Delta q_{max} \tanh\left[\frac{e\beta(V - V_h)}{2kT}\right] \quad (1)$$

$$\tau(V) = \tau_{max} \operatorname{sech}\left[\frac{e\beta(V - V_h)}{2kT}\right] \quad (2)$$

V_h, the membrane potential at which there are equal numbers of ions in each potential energy well, could differ from zero because of membrane asymmetry. β is the fraction of the externally applied potential effectively felt by the translocating ion; e is the charge on each ion, k and T are Boltzmann's constant and absolute temperature. Δq_{max} and τ_{max} are, respectively, the total charge in each energy well and the time constant for translocation, both at $V = V_h$. The smooth curve in Fig. 4 is the fit to Eq. 1 with Δq_{max} = 4770 ± 140 fC, β = 0.42 ± 0.02, and V_h = −3.8 ± 1.5 mV. Likewise the smooth curve in Fig. 5 is the fit to Eq. 2 with β constrained to 0.42. The best fit is with parameters τ_{max} =

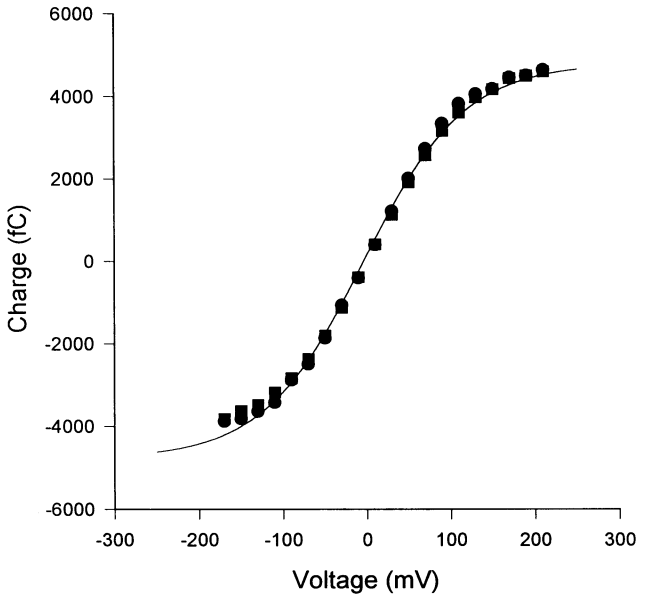

FIGURE 4 Voltage dependence of DiSBA-C_6-(3) moved during the displacement and tail currents for voltage changes from a −30 mV holding potential. The circles are the data from the on response and the squares from the tail currents. The raw data were fit to a single exponential and the charge moved, the area, was calculated as the product of the current amplitude and the time constant. The fit to Eq. 1 with Δq_{max} = 4770 fC, β = 0.42, and V_h = −3.8 mV is the solid curve.

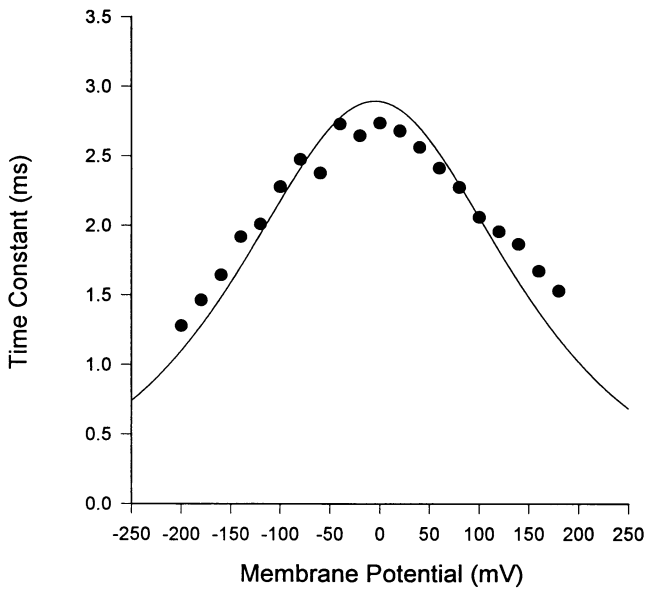

FIGURE 5 The voltage dependence of DiSBA-C_6-(3) displacement current time constants in L-M(TK$^-$) cells for the same data shown in Fig. 4. The fit to Eq. 2, with β = 0.42, τ_{max} = 2.9 ms, and V_h = −5 mV is the solid curve.

2.9 ± 0.06 ms and V_h = −5 ± 4 mV. These results demonstrate that the oxonol senses a significant part of the electric field across the membrane, translocates in ~3 ms or less, and that the greatest sensitivity and linearity of translocation as a function of membrane potential is in the physiologically relevant range. The reason why β is significantly less than 1 and why the fits are less accurate at extreme voltages is probably electrostatic repulsions between the charges within the membrane. In qualitative terms, any asymmetry in mobile charge distribution tends to produce an electrostatic repulsion opposing further increase in that asymmetry. The strength of this negative feedback increases with the charge density and the depth of ion burial in the membrane. Burial depths of only 4 Å can decrease the β parameter by a factor of 2 (Tsien and Hladky, 1982) at charge densities comparable to those here. β values of 0.63 have been determined from displacement currents of dipicrylamine and tetraphenylborate anions in squid axons and GH_3 cells, respectively (Fernández et al., 1983, 1984).

Voltage-dependent fluorescence resonance energy transfer

To transduce charge displacements into optical signals, the oxonol fluorescences at the intracellular and extracellular membrane binding sites must be made different. Fluorescence asymmetry is created with the introduction of fluorescently labeled lectins bound to the extracellular membrane surface. Excitation of FL-WGA leads to energy transfer to oxonols located in the extracellular membrane binding site as shown in Fig. 1. The extinction coefficient and the fluorescence quantum yield of FL-WGA was measured to be 222,000 M^{-1} cm^{-1} (~3 fluorescein/protein) and 0.23, respectively. In Jurkat cell suspensions labeled with FL-WGA, up to 30% of the lectin fluorescence intensity, was quenched upon titration of DiSBA-C_4-(3). In the best case, where all of the quenching is due to energy transfer, the average distance from the lectin to the membrane-bound oxonol is still greater than 50 Å, the calculated Förster distance R_0 for the FL-WGA/bis-(1, 3-dialkyl-2-thiobarbiturate) trimethineoxonol pair. The spectral overlap between the FL-WGA emission and DiSBA-C_6-(3) excitation is given in Fig. 2. Because FRET falls off with the inverse sixth power of the distance separating the two fluorophores, energy transfer to oxonols in the intracellular membrane site, an additional 40 Å away, is probably negligible.

Upon depolarization, the oxonol molecules redistribute such that more are bound to the intracellular site and less to the extracellular one. This change manifests itself with a decrease in the energy transfer, resulting in an increase in the fluorescence of the FL-WGA and a concomitant decrease in the oxonol emission. The fluorescence signals in a voltage-clamped L-M(TK$^-$) cell labeled with the DiSBA-C_4-(3)/FL-WGA pair (FLOX4) and depolarized with four increasing voltage steps are shown in Fig. 6. The FL-WGA emission increases 7–8%, the oxonol fluorescence decreases 10%, and the FL-WGA/oxonol emission ratio changes 19% for a 120 mV depolarization. The simultaneous changes in donor and acceptor emissions is consistent with the FRET mechanism outlined in Fig. 1. The decrease

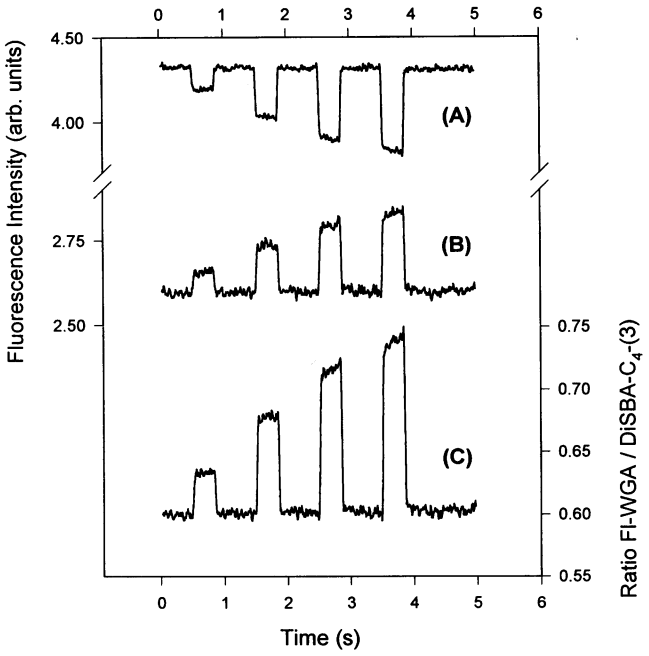

FIGURE 6 Simultaneous fluorescence changes of FLOX4 in response to four depolarizations from −70 mV of 40, 80, 120, and 160 mV in a L-M(TK⁻) cell at 20°C. The single wavelength fluorescence emission traces of DiSBA-C_4-(3) and FL-WGA are shown in *A* and *B*, respectively. The oxonol emission decreases and FL-WGA signal increases with depolarization. The FL-WGA/DiSBA-C_4-(3) ratio is displayed in *C*. The data are the average of 29 sweeps.

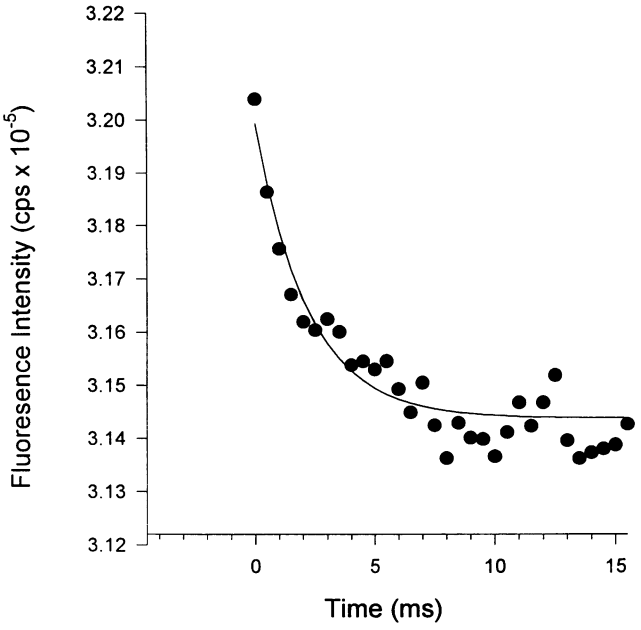

FIGURE 7 Time course of the fluorescence change of (*B*) DiSBA-C_{10}-(3) from FLOX10 in response to a 100 mV depolarization from −70 mV. The solid curve is a fit to a single exponential with a 2-ms time constant. The data is the average of 3 L-M(TK⁻) cells, at 20°C, acquired at 2 kHz.

in oxonol emission with depolarization is opposite to what is observed for the slow voltage-sensitive uptake of oxonols in cells (Rink et al., 1980). The fluorescence changes have time constants of ~18 ms at 20°C, in agreement with the DiSBA-C_4-(3) displacement currents. No large fluorescence changes are observed in the absence of FL-WGA. The translocation rate of DiSBA-C_4-(3) speeds up with increasing temperature. The time constant falls to 7–8 ms at 29°C, corresponding to an activation energy of ~17 kcal/mol. However, raising the temperature also increases internalization of the lectin and eventually decreases the fluorescence change. The oxonols with R = ethyl and butyl also reach internal cellular membranes, although active membrane internalization is probably not necessary. Additional dilution of the voltage-dependent FRET signals arises from spectral overlap of the fluorescein and oxonol, such that some of the light in the fluorescein emission channel comes from the oxonol, and vice versa.

Increasing the length of the alkyl chains on the oxonol improves the voltage response times significantly. The DiSBA-C_6-(3)/FL-WGA pair, FLOX6, has a time constant of ~3 ms at 20°C, whereas the DiSBA-C_{10}-(3)/FL-WGA pair, FLOX10, responds with a time constant of 2 ms, as shown in Fig. 7. The response in the figure is slightly slower than the true value because of smoothing. The fluorescence time constants are in agreement with those from the displacement currents, for example, in Fig. 3. The beneficial effect of adding hydrophobicity to the oxonol in the form of longer alkyl chains reaches a plateau. There is a large sixfold increase in translocation rate substituting hexyl for butyl on the oxonol core. However, the addition of twice as many methylene groups in going from the hexyl to the decyl compound results in less than a twofold increase. These faster translocating oxonols are essentially insoluble in water and require modified procedures to load into cells. DiSBA-C_6-(3) is easily loaded in normal medium supplemented with 1.5 mM β-cyclodextrin to complex the alkyl chains. Nonfluorescent DiSBA-C_6-(3) aggregates in HBSS become fluorescent upon addition of β-cyclodextrin. DiSBA-C_{10}-(3) requires loading in a medium of low ionic strength with osmolarity maintained with sucrose. Labeling is confined almost exclusively to the plasma membrane, presumably because the hydrophobicity is now great enough to prevent desorption from the first membrane the dye encounters. The direction of energy transfer can be reversed using TR-WGA instead of FL-WGA. DiSBA-C_6-(3) functions as a FRET donor to TR-WGA in L-M(TK⁻) cells with the same response time as FLOX6. The spectral overlap of this FRET pair is shown in Fig. 2. The signal change, however, is only one-half that for FLOX6. The limiting factor at present seems to be that the surface binding sites for the lectin are not dense enough on these cells for the TR-WGA to capture a large fraction of the donor excitation.

The FLOX6 system was tested in a variety of cell lines. In neonatal cardiac myocytes, the two fluorophores could be loaded without affecting the spontaneous beating. There-

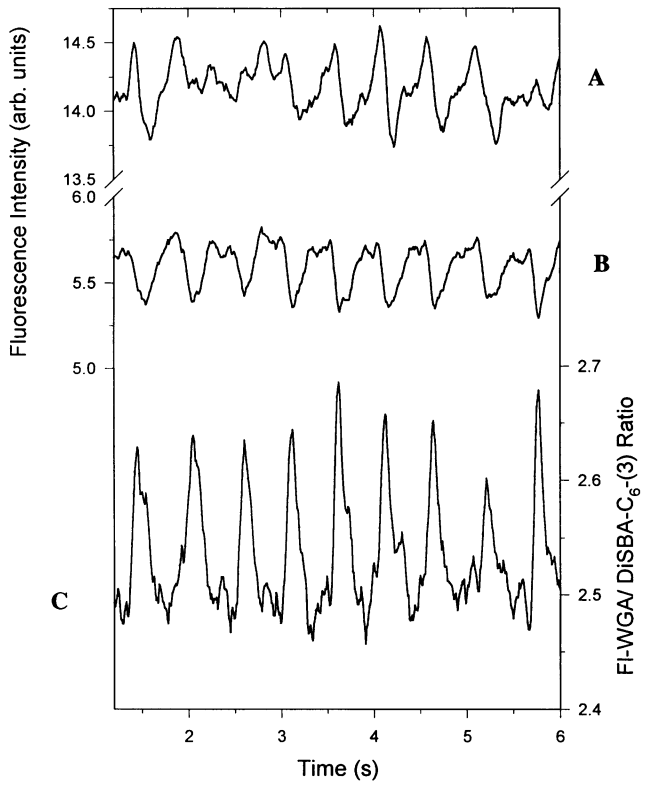

FIGURE 8 Single sweep trace of FLOX6 fluorescence ratio changes in beating neonatal cardiac myocytes. The top trace (*A*) shows the FL-WGA channel; (*B*) is the longer wavelength oxonol channel; and (*C*) is the FL-WGA/oxonol ratio, in which motion artifacts are significantly reduced. The data were acquired at 100 Hz and 10 μM of isoproterenol was added to the bath solution.

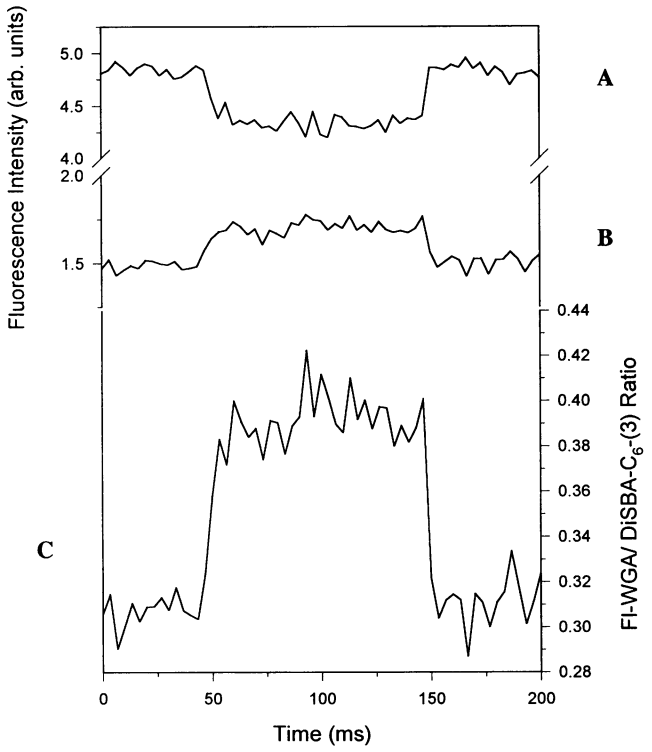

FIGURE 9 The fluorescence changes of FLOX6 in a voltage clamped astrocytoma cell. The top trace (*A*) is the DiSBA-C_6-(3) emission; (*B*) is the FL-WGA fluorescence signal; and (*C*) is the FL-WGA/oxonol ratio. After a 50-ms delay, the membrane potential was depolarized 100 mV from −70 mV for 100 ms. The traces are the average of four sweeps acquired at 300 Hz, with no smoothing. The time constant for the fluorescence changes is less than 3.3 ms consistent with the displacement currents, such as those in Fig. 3. A small background signal was subtracted from the starting signal, <5% for the oxonol channel and <15% for the fluorescein channel.

fore, the added capacitance from the oxonol displacement current did not prevent generation of action potentials. The periodic 90 mV action potentials (Conforti et al., 1991) could be observed in a single sweep (Fig. 8 *C*). The ratio change without subtraction of any background fluorescence was 4–8%. Motion artifacts were observed in the single wavelength data. In Fig. 8, *A* and *B*, large slow changes in the detected light were observed in both channels. Satisfyingly, these effects were essentially eliminated in the ratio data. The voltage-dependent fluorescence changes are faster than the mechanically based artifacts, as expected (Hill and Courtney, 1982). Some cells, loaded with oxonol at 2.3 μM, did stop beating after about 7 s of continuous exposure to the xenon arc illumination. At 0.6 μM loading, the phototoxicity and unfortunately the signal were reduced. In differentiated B104 neuroblastoma cells an 8% ratio increase was recorded, without any background subtraction, for a 120 mV depolarization. The inward sodium currents did not deteriorate from phototoxic effects during experiments with excitation exposures totaling 10–20 s. FLOX6-labeled 1321N astrocytoma cells showed oxonol and FL-WGA fluorescence almost exclusively on the plasma membrane. Ratio changes of 22–34% for 100 mV were observed in photometry experiments such as those in Fig. 9. The fluorescence intensities in the fluorescein and oxonol channels increased ~17% and decreased ~16%, respectively, for 100 mV depolarization. In these cells, unlike the L-M(TK$^-$), the cross-talk between emission channels was decreased and larger changes occurred in the fluorescein signal. These signal changes are the largest millisecond membrane potential dependent ratio changes observed in single cells. Previous investigations have shown that 4-ANEPPS gives a 9%/100 mV excitation ratio change (Montana et al., 1989). In addition, FLOX6's fluorescence changes in each emission channel are comparable to the largest reported changes, for example, the 21%/100 mV change in a neuroblastoma using RH-421 (Grinvald et al., 1983). The large FLOX6 signals allowed us to record images of voltage-clamped L-M(TK$^-$) and astrocytoma cells using a high-speed confocal microscope. The astrocytoma cells gave a 10–20% ratio increase that was localized to the plasma membrane for a 120 mV depolarization, as shown in Fig. 10. The apparent thickness of the plasma membrane staining is an artifact of smoothing and averaging 16 stimulus presentations during which slight motion of the cell occurred.

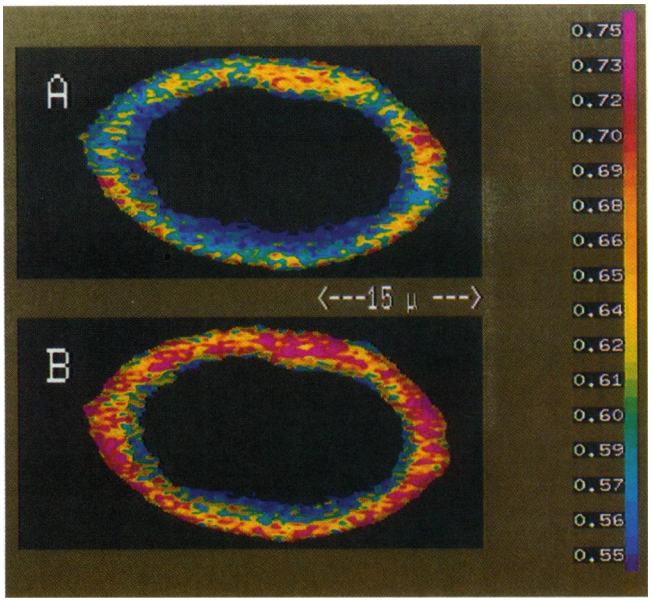

FIGURE 10 Confocal image of a voltage clamped astrocytoma cell at (*A*) −70 and (*B*) 50 mV, stained with FLOX6.

The voltage-sensitive fluorescence mechanism introduced in this paper offers both advantages and disadvantages compared with previously known mechanisms for optical sensing of potential (Loew, 1988, 1993, Waggoner and Grinvald, 1977). The biggest advantage is that a 60 mV change could give in principle up to a 10-fold change in concentration ratio of the mobile dye at the two membrane interfaces, with response times eventually in the submillisecond domain. The optical signals should be correspondingly large assuming that FRET and emission ratioing can distinguish the two populations of the mobile fluorophore. The present initial demonstrations fall short of this ideal because of practical limitations such as incomplete energy transfer between the lectin and the oxonol on the same side of the plasma membrane, fluorescence arising from sites other than the plasma membrane, cross-talk between the two emission bands, mutual repulsion between anions, and less than ideal speeds of anion translocation. Nevertheless, all of these problems should be isolable and at least somewhat amenable to rational amelioration, whereas comparable attempts to improve existing classes of dyes are no longer producing dramatic improvements. In addition, FRET using a fluorescent acceptor inherently offers an emission ratio change that is well suited to laser-scanning confocal microscopy and internally corrects for variations in donor loading, cell thickness and position (including motion artifacts), and excitation intensity. If emission ratioing is not desirable or possible, either wavelength can still be used alone, or the change in donor excited-state lifetime might be monitored. Finally, a potential advantage of this approach is that molecular specificity for particular cell types in a mixed population might be introduced by using cell-specific antibodies or adhesion molecules as the carriers of the extracellular fluorescent label. Specifically labeled cells would also reduce background fluorescence and maintain the large fluorescence changes in complex tissue. Background staining is a great problem in optical studies of the nervous system and typically causes the fractional fluorescence changes to be reduced at least an order of magnitude from those found in simple cells.

The FRET based mechanism does also have intrinsic disadvantages. The requirement for anion translocation will prevent response times below 10^{-5} to 10^{-4} s, whereas electrochromic mechanisms can work within the nanosecond lifetime of the excited state. However, only a small fraction of current neurobiological applications actually demand submillisecond fidelity. The motion of the mobile anions must generate a displacement current, which might represent a significant capacitative shunt in some cases. The obvious remedy is to use as low a loading of mobile anion as possible. To maintain a sufficient surface density of acceptors to give adequate energy transfer efficiency, it becomes theoretically preferable for the mobile anions to be the donors and the fixed labels to be the acceptors in stoichiometric excess, or to tie the two together with a tether long enough to span the entire membrane. The latter solution would pose nontrivial problems in chemical synthesis and tissue loading but should make the optical response characteristics independent of absolute acceptor concentration. Another inherent though minor disadvantage is that the responses deviate significantly from linearity and saturate for very large voltage changes. Some nonlinearity is inevitable in any really sensitive fluorescence mechanism because fluorescence can neither go negative nor increase without limit. Fortunately, the actual response, a hyperbolic tangent function of voltage, maximizes sensitivity over the physiologically most relevant range of membrane potentials and is mathematically tractable and correctable. Most current applications of fast potentiometric indicators do not attempt to calibrate absolute values of membrane potential. We believe that voltage indicators based on FRET may already be practically useful and that modest, rationally attainable improvements in sensitivity and speed could make them superior for many biological applications.

We would like to thank the following people: Brian Bacskai for his help in acquiring the confocal image; Aaron Fox for his assistance in writing the Axobasic acquisition program; and Stephen Adams and Gregor Zlokarnik for helpful discussions.

REFERENCES

Andersen, O. S., and Fuchs, M. 1975. Potential energy barriers to ion transport within lipid bilayer. *Biophys. J.* 15:795–830.

Benz, R. 1988. Structural requirement for the rapid movement of charged molecules across membranes. *Biophys. J.* 54:25–33.

Benz, R., and Conti, F. 1981. Structure of the squid axon membrane as derived from charge-pulse relaxation studies in the presence of absorbed lipophilic ions. *J. Membr. Biol.* 59:91–104.

Benz, R., P. Läuger, and Janko, K. 1976. Transport kinetics of hydrophobic ions in lipid bilayer membranes. *Biochim. Biophys. Acta.* 455:701–720.

Benz, R., and Nonner, W. 1981. Structure of the axolemma of frog myelinated nerve: relaxation experiments with a lipophilic probe ion. *J. Membr. Biol.* 59:127–134.

Bortnick, N., L. S. Luskin, M. D. Hurwitz, and Rytina, A. W. 1956. *t*-Carbinamines, RR′R″CNH_2. III. The preparation of isocyanates, isothiocyanates and related compounds. *J. Am. Chem. Soc.* 78:4358–4361.

Cohen, L. B., and S. Lesher. 1985. Optical monitoring of membrane potential: methods of multisite optical measurement. *In* Optical Methods in Cell Physiology. P. de Weer and B. M. Salzberg, editors. Wiley, New York. 71–99.

Conforti, L., N. Tohse, and N. Sperelakis. 1991. Influence of sympathetic innervation on the membrane electrical properties of neonatal rat cardiomyocytes in culture. *J. Dev. Physiol.* 15:237–246.

Fernández, J. M., A. P. Fox, and S. Krasne. 1984. Membrane patches and whole-cell membranes: a comparison of electrical properties in rat clonal pituitary (GH_3) cells. *J. Physiol.* 356:565–585.

Fernández, J. M., R. E. Taylor, and F. Bezanilla. 1983. Induced capacitance in the squid giant axon. *J. Gen. Physiol.* 82:331–346.

Flewelling, R. F., and W. L. Hubbell. 1986. The membrane dipole potential in a total membrane potential model. *Biophys. J.* 49:541–552.

Grinvald, A., A. Fine, I. C. Farber, and R. Hildesheim. 1983. Fluorescence monitoring of electrical responses from small neurons and their processes. *Biophys. J.* 42:195–198.

Grinvald, A., R. D. Frostig, E. Lieke, and R. Hildesheim. 1988. Optical imaging of neuronal activity. *Physiol. Rev.* 68:1285–1366.

Henderson, S. A., M. Spencer, A. Sen, C. Kumar, M. A. Q. Siddiqui, and K. R. Chien. 1989. Structure organization, and expression of the rat cardiac myosin light chain-2 gene. *J. Biol. Chem.* 264:18142–18146.

Hill, B. C., and K. R. Courtney. 1982. Voltage-sensitive dyes discerning contraction and electrical signals in myocardium. *Biophys. J.* 40: 255–257.

Hodgkin, A. 1975. The optimum density of sodium channels in an unmylinated nerve. *Phil. Trans. R. Soc. Lond. [Biol.].* 270:297–300.

Ketterer, B., B. Neumcke, and P. Läuger. 1971. Transport mechanism of hydrophobic ions through lipid bilayer membranes. *J. Membr. Biol.* 5:225–245.

Loew, L. M. 1988. How to choose a potentiometric membrane probe. *In* Spectroscopic Membrane Probes. L. M. Loew, editor. CRC Press, Boca Raton. 139–151.

Loew, L. M. 1993. Potentiometric membrane dyes. *In* Fluorescent and Luminescent Probes for Biological Activity. W. T. Mason, editor. Academic, San Diego. 150–160.

Montana, V., D. L. Farkas, and L. M. Loew. 1989. Dual-wavelength ratiometric fluorescence measurements of membrane potential. *Biochemistry.* 28:4536–4539.

Rink, T. J., C. Montecucco, T. R. Hesketh, and R. Y. Tsien. 1980. Lymphocyte membrane potential assessed with fluorescent probes. *Biochim. Biophys. Acta.* 595:15–30.

Salzberg, B. M. 1983. Optical recording of electrical activity in neurons using molecular probes. *In* Current Methods in Cellular Neurobiology. J. L. Barker, editor. Wiley, New York. 139–187.

Savitzky, A., and M. J. E. Golay. 1964. Smoothing and differentiation of data by simplified least squares procedure. *Anal. Chem.* 36:1627–1639.

Tsien, R. Y. 1976. Chemical tools in cellular physiology. Ph.D. thesis. University of Cambridge.

Tsien, R. Y., and B. J. Bacskai. 1995. Video-rate confocal microscopy. *In* Handbook of Biological Confocal Microscopy. 2nd ed. J. B. Pawley, editor. Plenum Press, New York. 459–478.

Tsien, R. Y., and S. B. Hladky. 1982. Ion repulsion in membranes. *Biophys. J.* 39:49–56.

Waggoner, A. S., and A. Grinvald. 1977. Mechanisms of rapid optical changes of potential sensitive dyes. *Ann. N. Y. Acad. Sci.* 303:217–241.

Weber, G., and F. W. K. Teale. 1957. Determination of the absolute quantum yield of fluorescent solutions. *Faraday Soc. Trans.* 53: 646–655.

Wu, P., and L. Brand. 1994. Resonance energy transfer: methods and applications. *Anal. Biochem.* 218:1–13.